ROSA/LSTF Experiments on PWR Natural Circulation and Validation of RELAP5/MOD3.3

Taisuke YONOMOTO

Japan Atomic Energy Research Institute

Abstract. Two steady-state natural circulation (NC) tests conducted at ROSA/LSTF at pressure of 7 and 0.1 MPa are summarized in this paper to show the estimated NC behavior in the Westinghouse type PWR in a wide range of pressure condition. The high-pressure NC test has indicated qualitatively the same NC modes of single-phase NC, two-phase NC, and reflux condensation as observed in smaller scale facilities depending on the primary side mass inventory. Because of large numbers of instrumentation points and U-tubes of LSTF, detailed flow modes and their effects on the loop flow were clarified; e.g., the loop flow during the two-phase NC was stable although intermittent flow occurred in a U-tube. Characteristic results observed only in the low-pressure test includes nonuniform flow among U-tubes consisting of two-phase vertical stratification and concurrent condensing flow. Observed stable two-phase stratification indicates that condensation is balanced with evaporation in one U-tube, which is affected by the secondary side temperature distribution that is typical of low pressure. The tests were analyzed using the RELAP5/MOD3 code with a simple or detailed noding model to represent SG U-tubes. The analyses results especially using the detailed model agreed well with observed stable loop flow behavior, transitions of the NC modes and the minimum mass inventory for steady-state heat removal. The code validation results using the low-pressure NC test data have shown the stable loop flow cannot be predicted just by increasing the number of the flow channels for the SG primary side because loop-to-loop oscillations that are not observed in the test occurs in the calculation.

1. Introduction

Because of the significance of natural circulation (NC) as a means to remove the decay heat from the core, many NC tests were conducted at the integral test facilities simulating the PWR including the SEMI-SCALE, LOFT, LSTF, BETHSY, LOBI, SPACE and so on. Those data were taken mainly in the eighties after the TMI accident for the validation and improvements of the analysis codes such as RELAP5. Since the research emphasis was placed mainly on the decay heat removal during small break loss-of-coolant accidents in the eighties, the NC tests were conducted mainly at high pressure at those facilities. On the other hand, a low pressure NC heat removal is also important for some kinds of new reactor designs including APWR+, a Mitsubishi developed reactor for the near term employment described in the previous section, to establish more robust heat removal systems.

The present paper summarizes the results on high (~7MPa) and low pressure (~0.2 MPa) NC experiments conducted at the ROSA/ Large Scale Test Facility (LSTF) [1]. The LSTF is a full-height and full-pressure thermal-hydraulic simulator of the Westinghouse type PWR with a volumetric scaling factor of 1/48. Then, the validation results of the RELAP5/MOD3.3 code are described to clarify the capability and limit of the code to reproduce the measured behavior[2]. Although the code has been validated by using the high pressure NC data obtained at the several PWR test facilities, the validation using the low pressure NC data is reported only by JAERI[3,4,5,6]. Furthermore, the comparison between the MOD3 and MO2 code results are described to clarify the improvements of the code model added to the MOD3.

2. Description of experiments

2.1. Test facility

The LSTF was built originally as a 1/48 volumetrically-scaled, full-height, full-pressure simulator of the current-generation Westinghouse-type four-loop (3423 MW thermal power) PWR. The core is simulated by a 10 MW electric heater rod assembly which consists of ~1000 heater rods of the same diameter and pitch as those of the reference PWR. The four loops of the reference PWR are lumped into two model loops (see Fig. 1). Each loop has a SG consisting of 141 full-size (19.6 mm i.d.) inverted-U-tubes with 9 different tube heights, a reactor coolant pump, a hot leg and a cold leg. Among the 141 U-tubes per SG, six are instrumented with bottom-to-top differential pressure measurements for both upflow and downflow sides of the tube, and with fluid and tube-wall thermocouples.

2.2. Test procedure and conditions

The steady-state NC tests are usually conducted at LSTF changing the primary mass inventory as a test parameter, and keeping the other parameters such as core power, the SG pressure, and SG liquid level to be at specified values. The primary mass inventory is reduced stepwise after observing steady-state behavior for several minutes at each mass inventory. The primary pressure is controlled using the electric heaters in the pressurizer only for the initial liquid single-phase condition. After the primary mass is reduced from the initial condition, the pressurizer is isolated by closing a valve in the pressurizer surge line to avoid the effects of the heat loss from the pressurizer. The observation of the steady NC behavior is continued until the core becomes exposed to steam environment and thus the stable core cooling becomes impossible.

In this paper, two tests are described to introduce typical NC behavior at high- and low- pressure. The specified secondary side pressure and core power were 6.6 MPa, and 1.4 MW for the high pressure NC test (ST-NC-02), and were 0.14 MPa and 0.94 MW for the low pressure NC (ST-NC-17). Here, the power of 1.4 MW corresponds to 2% of the nominal core power. Each test consisted of ~15 steady state conditions by discharging approximately 5% of the primary mass when the inventory condition was changed. Here, 100 % mass inventory is defined as the primary mass inventory for the initial liquid single-phase condition, excluding the pressurizer mass inventory.

2.3. High pressure test results

The NC flow behavior at high-pressure has been investigated at several PWR simulation test facilities, and is generally recognized that there are three heat transfer modes, depending on the primary mass inventory, of single-phase NC, two-phase NC and reflux condensation. The reflux condensation mode is characterized by the heat transfer through vapor generation in the core and condensation in the SG U-tubes. Half of the condensate returns to the core through the hot leg, and the other circulates through the loop seal and cold leg. The transition to the two-phase NC from the single-phase NC occurs when the liquid level in the upper plenum decreases to the hot leg elevation and then the vapor produced in the core starts to flow into the hot legs. The transition to the reflux condensation occurs when the liquid carry over becomes impossible across the inverted U-tube top.

The measured response of NC flow rates to the primary mass inventory change is shown in Fig.2, which were similar to those obtained in the smaller test facilities. The figure shows that the transitions to the two-phase NC and to the reflux condensation occurred at ~90% and ~60%, respectively. The maximum flow rate was observed at 77% mass inventory.

Various kinds of flow behavior were observed among SG U-tubes as summarized in Fig.3. They were classified into eight different flow modes: 1) single-phase liquid normal flow, 2) single-phase liquid reversed flow, 3) liquid continuous two-phase concurrent normal flow, 4) two-phase reversed flow, 5) cyclic fill and dump, 6) reflux condensation above two-phase mixture, 7) reflux condensation without liquid holdup, 8) reflux condensation with oscillatory liquid holdup[7].

The nonuniform flow characterized by the coexistence of the normal and reversed flow was observed for the mass inventory between 100 and 75%. Qualitatively, flow reversal tended to occur preferentially in the longer tubes when the SG outlet plenum pressure was higher than the inlet plenum pressure. The mechanism of this type of nonuniform flow with the reversed flow is discussed in several papers including Ref.7. For a given positive pressure difference between the outlet and inlet plenum, there exists three solutions for the U-tube flow rate corresponding to stable positive, unstable positive and stable negative flow rates. When the average flow rate in the U-tube fells into the unstable region, the flows inside the U-tubes change into either the positive stable flow or negative one so that the unstable flow can be avoided.

Another characteristic behavior observed during tests was the fill and dump mode, which was not observed for the low-pressure test as will be mentioned. The fill and dump process is repeated more or less periodically as illustrated schematically in Fig.4. A filling period continued for typically 100 s, followed by a quick dump of fluid into the tube downflow side. During the filling period, mixture/liquid levels increase in both sides of the tube as the vapor plug in the tube becomes smaller due to condensation. A quick dump of the mixture into the downflow side occurs when the mixture level in the upflow side reaches the top of the U-bend. Since the fill and dump mode occurs out of phase among U-tubes, the loop flow rate is not directly affected by the intermittent flow in a U-tube, that is, the fluctuation of the loop flow rate is relatively small.

2.4. Low pressure test results

2.4.1. Overall Behavior

The measured NC flow rate vs. the primary mass inventory is shown in Fig.2 for the low pressure test, compared with the high-pressure test result. In comparison with the high pressure test results, the reflux condensation mode started at lower mass inventory of ~40%, and the NC flow rate was larger for the mass inventory of less than 70%. These quantitative differences are caused by pressure effects; vapor flow rate is, in general, higher for a given core power with the decrease in pressure, which results in the larger interfacial drag and thus, larger carryover across the U-tube top. This causes the continuation of the two-phase NC down to smaller mass inventory for the low-pressure test.

Flow behavior observed only for the low-pressure test was a system-wide oscillation for the mass inventory between 40 and 50%. This flow behavior is characterized by intermittent changes of the loop flow, and oscillations of the liquid levels in the pressure vessel and SG outlet plenum with a typical time period of ~100 s as shown in Fig.5. In each cycle, the loop flow is stagnated for a time period of ~60 s, followed by the sudden increase of the flow lasting for ~40 s. The oscillations were in phase between the two loops. This intermittent behavior was caused by the oscillations in the loop flow, core vapor generation, and carryover across the U-tubes top. The intermittent loop flow was caused by the intermittent carryover, which was caused by the oscillatory core vapor generation, which was caused by the intermittent loop flow rate. Since the effect of a cause appeared with a relatively long delay time determined by the thermal inertia and the fluid transport time, these processes became oscillatory.

The fluid temperatures in the SG secondary side showed a characteristic C-shape vertical distribution; the temperature was subcooled and increased with elevation in the lower part, saturated and taking the maximum around the midplane, and decreasing with elevation due to the decrease in the saturation temperature (see Fig.6). The fluid subcooling occurred because of the circulation in the SG secondary side. That is, the saturated liquid from the separator flowed into the downcomer, and entered into the bottom of the boiling region where the saturation temperature was higher due to the water head. This temperature distribution caused several characteristic behaviors at low pressure, when compared to high-pressure NC behavior where the secondary side temperatures are typically saturated and uniform.

2.4.2. Non-uniform Behavior among U-tubes

Several flow modes were also observed among U-tubes for the low-pressure test as shown in Fig.7. At 100% mass inventory, the fluid temperatures in the instrumented tubes were almost the same as those at the same elevation in the secondary side, indicating flow stagnation and no heat transfer. All the instrumented U-tubes were, therefore, classified as "liquid single-phase flow stagnation" in Fig. 7, although there should be some U-tubes with non-zero flow because relatively stable loop flow was measured at the pump suction.

For the primary mass inventory between 64% and 91%, two flow modes were observed: "two-phase condensing flow mode" and "two-phase stratification mode." In the U-tube classified as "two-phase condensing flow mode," the fluid temperatures decreased in the flow direction and were higher than the secondary temperature throughout the U-tube. These are indications of the existence of the heat transfer and flow inside the tube. On the other hand, for the tube classified as "two-phase stratification," the fluid temperatures below the mixture level were roughly the same as those in the secondary side temperatures especially for the mass inventory between 91 and 80%. This suggests that the two-phase flow did not enter into these U-tubes from the inlet plenum, and the stable vapor space was present in the tube, as illustrated in Fig.8. For the inventory between 75 and 64%, fluid saturation was observed in the lower part of the inlet side of the stratified U-tubes, suggesting the ingress of the two-phase flow. The magnitude of the ingress was not significant as indicated by continuous fluid subcooling measured in the lower part of the downflow side of these U-tubes.

At the mass inventory of 59%, the U-tube downflow side became almost empty of liquid and the liquid level was formed in the SG outlet plenum. The two-phase stratification became less evident for most of instrumented U-tubes, that is, the fluid saturation was observed in the lower part of the down flow side. The loop flow became more oscillatory, but was still continuous, which suggests that the liquid carryover in each U-tube occurred oscillatory in out-of-phase among U-tubes.

With further decreasing the mass inventory, the loop flow rate became intermittent, suggesting that the liquid carryover to the downflow side of the U-tube was intermittent and in-phase among U-tubes (see Figs.5 and 8). When the mass inventory further decreased to 38%, the upflow side of U-tubes also became empty of liquid and the "reflux condensation mode" began.

When compared to typical high-pressure tests conducted in several PWR integral facilities, the most important difference is the existence of "two-phase stratification." The "fill and dump mode" has been observed during the two-phase NC at high pressure.

The above-mentioned difference in the U-tube flow behavior is caused by the difference of the secondary side temperature distributions. Since the secondary fluid temperature in the U-tube top region was relatively cold as shown in Fig.6, the condensation occurred therein. Nevertheless, the vapor plug was stably existed in the tube. This means that the decrease of vapor mass due to condensation was balanced with the vapor generation due to boiling occurring around the midplane where the secondary side temperature was relatively high. This speculated behavior has been confirmed in the SG analysis using the RELAP5 code as will be mentioned later. On the other hand, the coexistence of vapor generation and condensation in one tube is impossible to occur at high pressure where the secondary side temperature is typically uniform.

3. Discussion on U-tube nonuniform flow observed in the low pressure test

The U-tube flow behavior at low pressure was analyzed using the RELAP5/MOD3.2 code to have better understanding on the observed nonuniform behavior characterized by the coexistence of two-phase condensing flow and vertical stratification. For this analysis, one U-tube was modeled using the pipe component with 32 calculation cells. The boundary conditions were based on the test data at 70% inventory, including the primary pressure and SG secondary side temperatures.

Figure 9 shows the volumetric vapor generation rate in the tube obtained in the two-phase stratification analysis. Stable liquid columns were calculated both in the upflow and downflow sides of tubes due to the balanced vapor generation and condensation inside the tube. This result confirms the previously-mentioned mechanism for the two-phase stratification mode, which is possible only when the pressure is of the same order of the static head.

The flow characteristics for the two-phase condensing flow were calculated by changing the inlet mass flux while fixing the other conditions. The results are shown in Fig.10, where the inlet flow rate is normalized by the tube flow rate assuming the uniform distribution among U-tubes. Note that the flow behavior was very oscillatory for the normalized flow of 1. For this condition, the vapor inlet flow rate was so small, compared to the possible condensation rate, that the pressure could not be maintained at a constant level, which resulted in the unstable flow including the reverse flow. With increasing the flow rate from 1, the differential pressure first decreased, showing a negative slope in the characteristic curve, and then increased. The negative slope was produced because the void fraction in the upflow side increased with increasing the mass flow rate. Such a flow is known to be unstable due to "flow excursion type" instability. The slope in the characteristic curve became positive when the upflow side became fully voided and the effect of the flow resistance increased. The flow behavior was relatively stable for the normalized flow rate between 4 and 8. Above the normalized flow rate of 8, all the vapor did not condense in the U-tube.

The above analyses have made clear that there are two stable flow modes for a given pressure difference between the inlet and outlet, corresponding to the two-phase stratification and concurrent condensing flow, when the uniformly distributed flow is in the unstable flow region. This causes the flow separation to avoid the unstable flow, and thus the nonuniform flow observed in the tests.

4. System analysis using the RELAP5/MOD3.3 code

The above-mentioned NC tests were analyzed using the RELAP5/MOD3.3 code to validate the ability of the code to predict the NC behavior at high and low pressure, focusing on the observed nonuniform behavior among U-tubes. Two input models with different SG noding models were, therefore, used for the analysis. For a simple noding case, U-tubes are modeled with one pipe component having eight nodes, which is a typical noding for the usual PWR analysis. The other model used nine pipe components each with ~34 nodes to represent U-tubes. The nine-tubes model corresponds to the nine U-tube types having different length among 141 tubes per a SG at LSTF. In total, the one-tube model consisted of ~240 volumes and ~200 heat structures to represent both the primary and secondary sides of the LSTF. On the other hand, ~800 volumes and ~760 heat structures were used for the nine-tubes model. The secondary-side pressure, collapsed liquid level, and feedwater temperature were controlled to match the experimental data for each steady-state condition by using the control components of the code.

4.1. Analysis results for high pressure tests

The comparison of the NC flow rates is shown in Fig.11 for the high pressure test, for which the SG primary side was modeled with a single pipe component (one-tube case) or 9 pipe components (nine-tubes case). Each plot point in the figure has a vertical bar, which corresponds to the standard deviation indicating the magnitude of the time-fluctuation of the measured or calculated result. For both cases, the code predicted well the overall behavior including the transitions to the two-phase NC and to the reflux condensation, and the minimum mass inventory for the steady cooling of ~30%. In detail, the loop flow rates were overpredicted for the mass inventory of larger-than 70%; e.g., the maximum flow rate was overpredicted by ~30%. The cause of the overprediction was discussed previously in the reference[8], which indicated that the overprediction was caused by the underprediction of the flow resistance in the U-tube, and the maximum flow rate agreed well with the data by blocking 40 % of the U-tubes[8]. The reverse flow was calculated in one tube component, equivalent to 15 % of U-tubes for 83% inventory in the nine-tube case (see Fig.12). This magnitude of reverse flow was not sufficient to reduce the loop flow rate as shown in minor improvement by the nine-tubes model over the one-tube model.

A considerable improvement by the use of the nine-tubes model is indicated in the 73 % inventory calculation. The calculated loop flow rates showed oscillation with the amplitude of ~25 kg/s and the period of ~200 s for the one-tube case and were stable for the nine-tubes case as shown in Fig.13. For the one-tube case, the oscillation in the U-tube directory affected the loop flow rate. For the nine-tubes case, the flow in each U-tube was oscillatory with the phase divided into two groups having a 180 degree difference each other, which resulted in the stable loop flow (see Fig.14). Although this calculated U-tube flow behavior was not completely the same as the experimental results showing the out-of-phase oscillation among U-tubes, much better agreements were obtained for the loop flow rate by using the nine-tubes model.

4.2.Analysis results for low pressure tests

The calculated time-averaged NC flow rates agree well with the experimental data both for the one-tube and nine-tubes cases as shown in Figs.15 and 16. The calculated flow rate vs. time, however, significantly disagreed with the data showing unrealistic loop-to-loop oscillations (see Figures 17 thorough 19). The calculated loop-to-loop oscillations had different time periods between the two cases: ~100 s for the one-tube case and ~300 s for the nine-tubes case. In each calculated cycle of the loop flow oscillation, the stable loop flow was partially calculated for ~150 s only for the nine-tubes case. The U-tube flows were also stable during this time period, showing stable nonuniform flow consisting of four tube components with condensing flow and five tube components with flow stagnation (see Fig.20). This can be regarded as an improvement by the use of the nine-tubes model, since the loop and U-tube flow were always oscillatory for the one-tube case.

These results suggest the prediction may be improved if the loop-to-loop oscillation is suppressed for the nine-tubes model. One of the possible causes of the loop-to-loop oscillation may be the noding of the SG secondary side. Since the SG boiling section is modeled with one pipe component, a disturbance in one U-tube causes instantaneous overall change in the SG secondary side behavior, causing the synchronized change in the other U-tube flow behavior. In future, the effects of the SG secondary side noding will be investigated.

The figure 21 compares the system pressures between the measured and calculated cases. Since the 100% mass inventory case could not be calculated by using the same pressure as the experimental data, the comparison is omitted. In general, the primary pressure is overpredicted by ~30 kPa, suggesting the overprediction of the heat transfer resistance at SG. This disagreement can be significant depending on the system design. For example, when the system has a gravity-driven injection system (GDIS) with the SG cooling system, the prediction of the primary pressure is important for the evaluation of the GDIS flow rate since the GDIS behavior is significantly affected by the pressure near the containment pressure.

5. Comparison with the REALP/MOD2 Results

When the test ST-NC-02 was conducted and analyzed in the eighties at LSTF, the data was used to validate the RELAP5/MOD2 code. Several disagreements were found in the comparison study, which includes[8]:

1) The maximum loop flow rate was overpredicted by ~30%

2) The core dryout was observed for the mass inventory of ~50% vs. 30% for the test

3) The loop flow was oscillatory for the mass inventory of ~70%

In order to find a cause of the problem 1), the SG primary side flow area was adjusted in the sensitivity calculations, since the other possible sources of the disagreements such as the core void fraction are not found to be large enough. The results indicated that the maximum flow matched the data by blocking 40 % of U-tubes. The present results showed the same disagreements as mentioned before. The results with the nine-tube models were slightly improved over those with the one-tube model, but the magnitude of the improvement were not satisfactory.

The problem 2) was improved significantly by the MOD3 calculation, probably due to the change in the junction interfacial drag calculation model. In MOD2, the junction friction factor was the average of those in the adjacent two volumes. For this procedure, the friction of the junction connecting horizontal and vertical volumes tends to have a value similar to that in the vertical volume, because the interfacial friction in the vertical volume has generally much larger value than the horizontal one. This caused the unrealistic liquid hold up in the hot leg riser section and the SG inlet plenum, which caused earlier core dryout in the calculation. For the MOD3 calculation, much larger weight is given to the upstream volume value to determine the junction value. The primary mass distribution was, therefore, predicted well, which contributed the improved prediction of the dryout mass inventory by the MOD3.

The problem 3) was just a noding problem as indicated in the present study. The increase in the number of the parallel channels for the SG primary side is proved to be a good remedy for this problem.

6. Conclusions

Two steady-state natural circulation (NC) tests conducted at ROSA/LSTF at pressure of 7 and 0.1 MPa are described in this paper to show estimated NC behavior in the Westinghouse type PWR in a wide range of pressure condition. The tests were analyzed using the RELAP5/MOD3 code with simple or detailed noding model, denoted one-tube or nine-tubes model, to represent SG U-tubes. The test and code validation results are summarized as follows:

1) The high-pressure test has indicated NC modes of single-phase NC, two-phase NC, and reflux condensation as observed in smaller scale facilities. Because of large number of instrumentation points and U-tubes of LSTF, detailed flow modes and their effects on the loop flow were clarified; eight flow modes were observed in the U-tube depending on the primary mass inventory, and the loop flow during the two-phase NC was stable although intermittent flow occurred in a U-tube.

2) The low-pressure test has shown a system-wide intermittent oscillation phase in between the two-phase NC and reflux condensation phases, which is characterized by the oscillations of the core void fraction, SG outlet plenum liquid level and loop flow with a typical time period of ~100 s. Characteristic SG primary side flow behavior observed only in the low-pressure test includes nonuniform flow among U-tubes consisting of two-phase stratification and concurrent condensing flow. The observed stable two-phase stratification indicates that condensation is balanced with

evaporation in one U-tube, affected by the secondary side temperature distribution that is typical of low pressure NC condition. Since the U-tubes with the two-phase stratification do not contribute heat transfer significantly, the nonuniform behavior reduces the effective heat transfer area between the primary and secondary side.

3) The RELAP5/MOD3 analysis using the SG partial model has confirmed that two stable flow modes of the two-phase stratification and the concurrent condensing can exist under the same U-tube pressure boundary conditions at low pressure, suggesting the mechanism of the nonuniform flow.

4) The RELAP5/MOD3 analyses results especially using the nine-tubes model agree well with the overall behavior observed in the high-pressure test including the transitions to each NC phase and the minimum mass inventory for the steady core cooling. The maximum loop flow was, however, overpredicted by ~30% due probably to the underprediction of the reverse flow rates in the SG primary side. Significant improvement using the nine-tubes models were observed in the calculation for the mass inventory of ~73%: stable loop flow was predicted by the nine-tubes model as observed in the test, and the oscillation was predicted with the one-tube model. This suggests some requirements for the SG input noding are needed to predict realistically the NC loop flow behavior.

5) The RELAP5/MOD3 validation results using the low pressure NC test data have shown the stable NC loop flow observed in the test was not predicted well just by increasing the number of the parallel flow channels in SG: loop-to-loop oscillations were calculated, which were not observed in the test. Although calculated U-tube flow was always unstable with the one-tube model, stable nonuniform flow consisting of the condensing flow and flow stagnation among U-tubes was partially calculated in each cycle of the loop-to-loop oscillation using the nine-tubes model. This suggests that suppressing the loop-to-loop oscillation in the nine-tubes models improves the prediction significantly.

6) The minimum mass inventory required for the steady-state core cooling was predicted well using the RELAP5/MOD3 code due to the change in the junction interfacial drag model, although it was not predicted by the RELAP5/MOD2.

REFERENCES

[1] ROSA-IV Group, "ROSA-IV Large Scale Test Facility (LSTF) system description for second simulated fuel assembly," JAERI-M90-176 (1990).

[2] RELAP5 Development Team, "RELAP5/MOD3 Code Manual," NUREG/CR-5535, INEL-95/0174, 1~4 (1995).

[3] Yonomoto, T., Kondo, M., Kukita, Y., "PWR small break loss-of-coolant-accident experiment at ROSA-V/LSTF with a combination of secondary-side depressurization and gravity-driven safety injection," J. Nucl. Sci. Tech., 34(6) (1997) pp.571-581.

[4] Yonomoto, T., Ohtsu, I., Anoda, Y., "Thermal-hydraulic characteristics of a next-generation reactor relying on steam generator secondary side cooling for primary depressurization and long-term passive core cooling," Nucl. Eng. Des., 185 (1998) pp.83-96.

[5] YONOMOTO, T., AND ANODA, Y., "Thermal-hydraulic research on next generation PWRs using ROSA/LSTF," IAEA-TECDOC- 1149, Proc. of 1998 IAEA tech. mtg. on experimental tests and qualification of analytical methods to address thermohydraulic phenomena in advanced water cooled reactor, Paul Scherrer Institute, Villigen, Switzerland, Sep. 14-17 (1998)

[6] Yonomoto, T., Ohtsu, I., "ROSA/LSTF Experiments on low-pressure natural circulation heat removal for next-generaiton PWRs, " Proc. 12th Pacific Basin Nucl. Conf. (2000) pp.317-329.

[7] KUKITA, Y., NAKAMURA, H., AND TASAKA, K., "Nonuniform steam generator U-tube flow distribution during natural circulation tests in ROSA-IV Large scale test facility", Nucl. Sci. Eng., 99 (1988) pp.289-298.

[8] Chauliac, C., Kukita, Y., Tasaka, K., "Post-test analysis with RELAP5/MOD2 of ROSA-IV/LSTF natural circulation test ST-NC-02", JAERI-M 88-215 (1988).

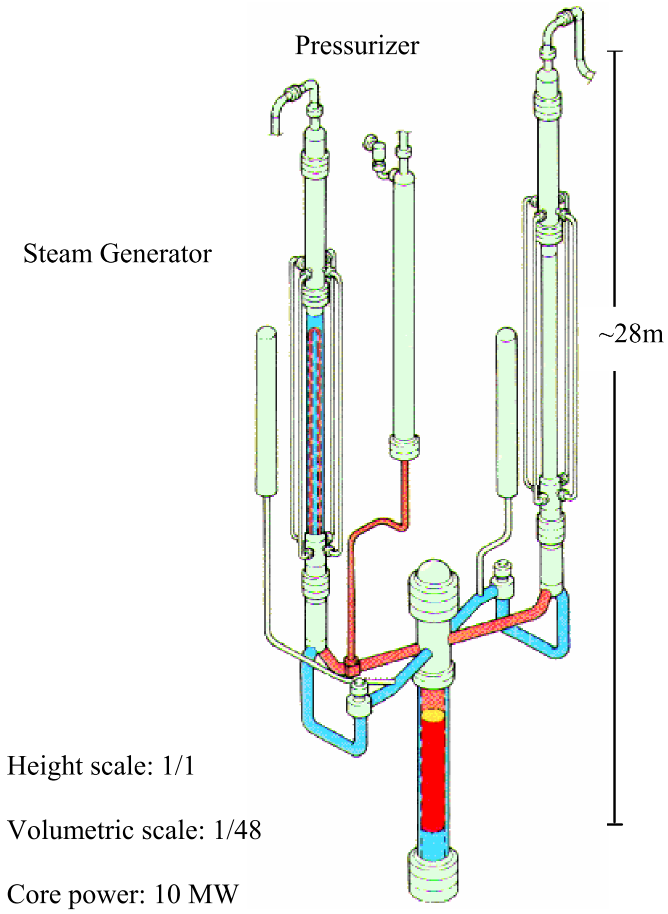

Fig.1 ROSA/LSTF

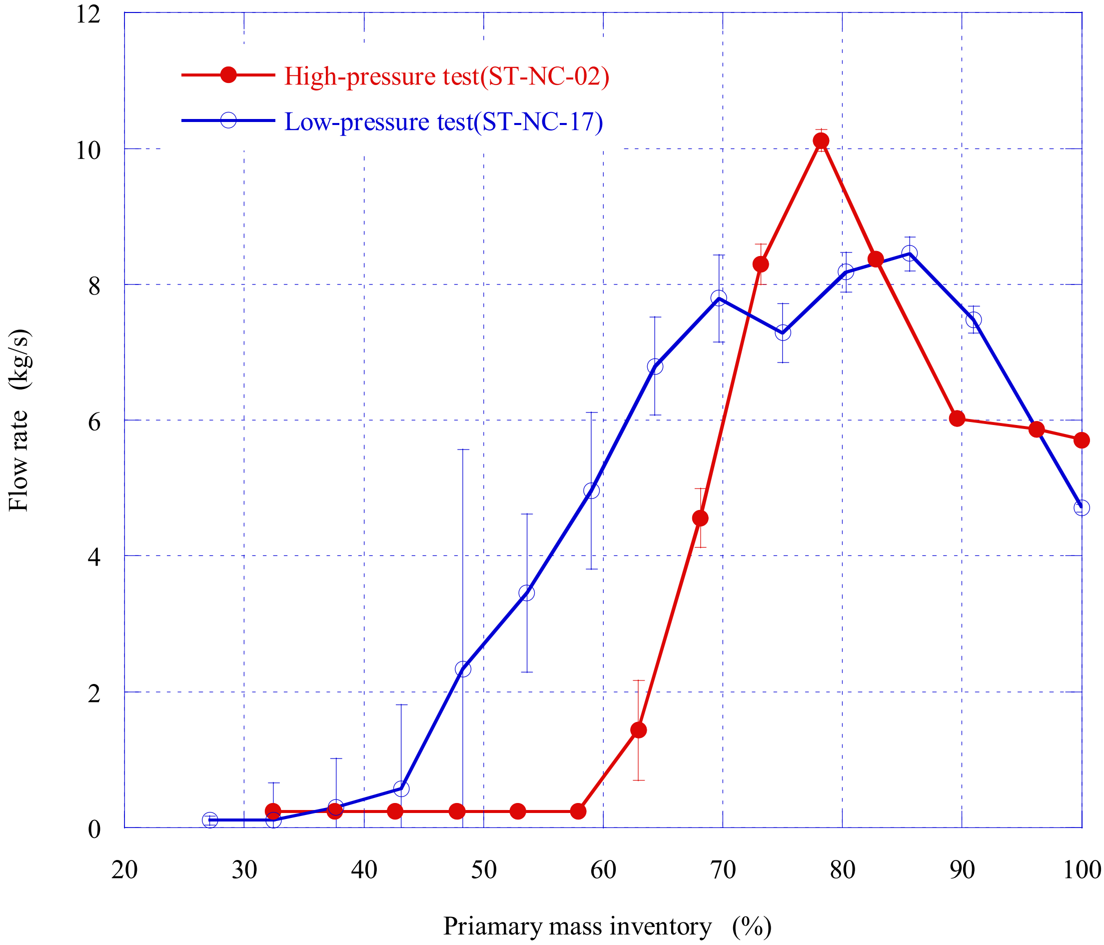

Fig.2 Measured loop flow rates vs. primary mass inventory: loop flow rates are measured at the pump suction.

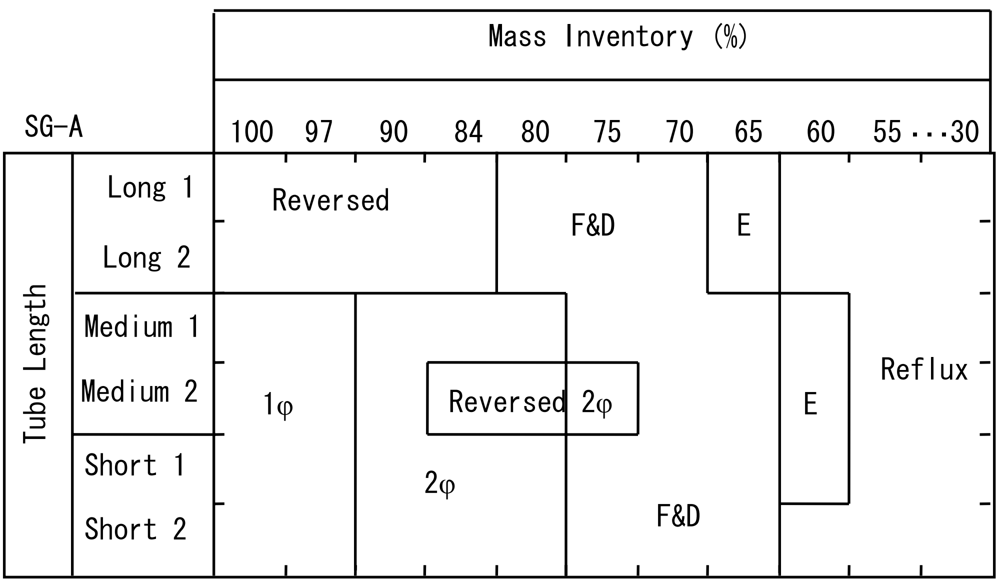

Fig.3 U-tube flow modes in SG-A versus primary system mass inventory for high pressure test(ST-NC-02): 1φ=single-phase normal flow; 2φ=liquid continuous two-phase normal flow; F&D=cyclic fill and dump, E=tube emptying, vapor and mixture regions coexist in the tube, Reversed indicates single- or two-phase low, and reflux indicates reflux condensation in empty tube.

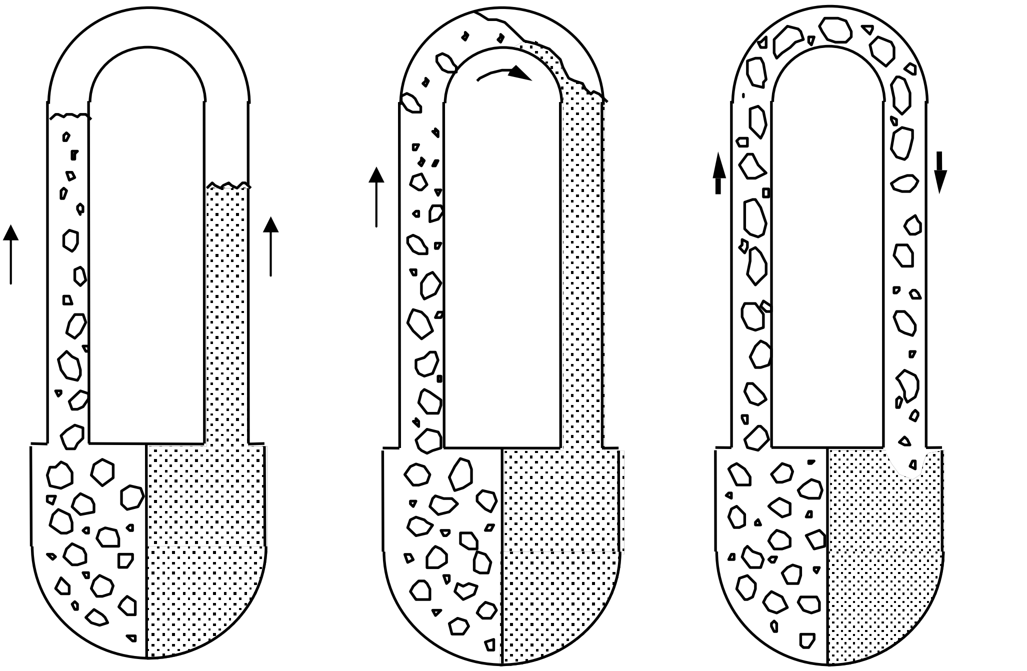

(a) Fill (b) Onset of dump (c) Two-phase carryover

Fig.4 Cyclic fill and dump in U-tube

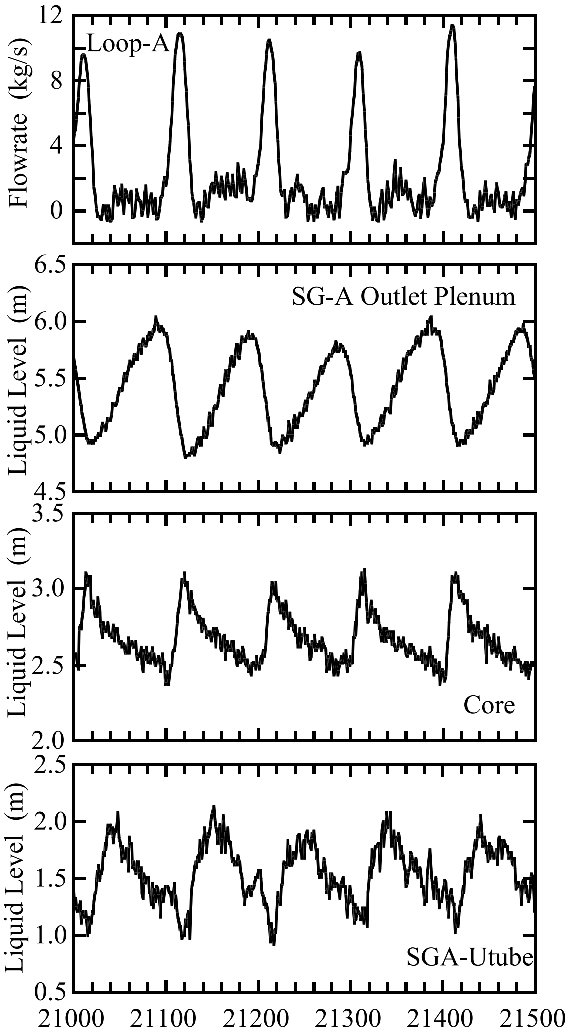

Fig.5 System-wide intermittent natural circulation behavior observed in low-pressure test

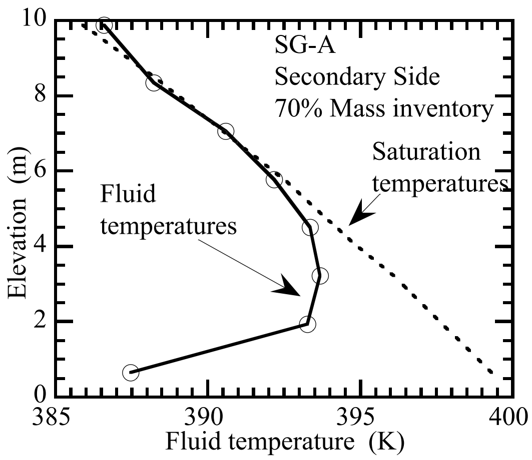

Fig.6 Fluid and saturation temperatures in the SG secondary side for low-pressure test

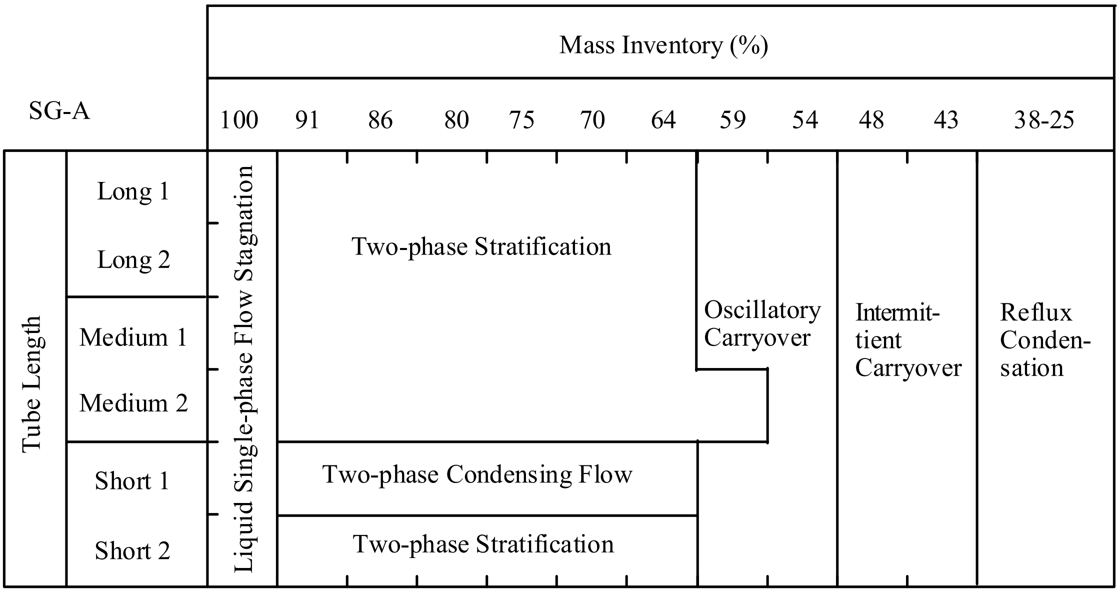

Fig.7 Observed flow modes among U-tubes vs. mass inventory: Long, Medium, and Short mean instrumented U-tubes with height of 11m, 10m, and 9.5 m, respectively.

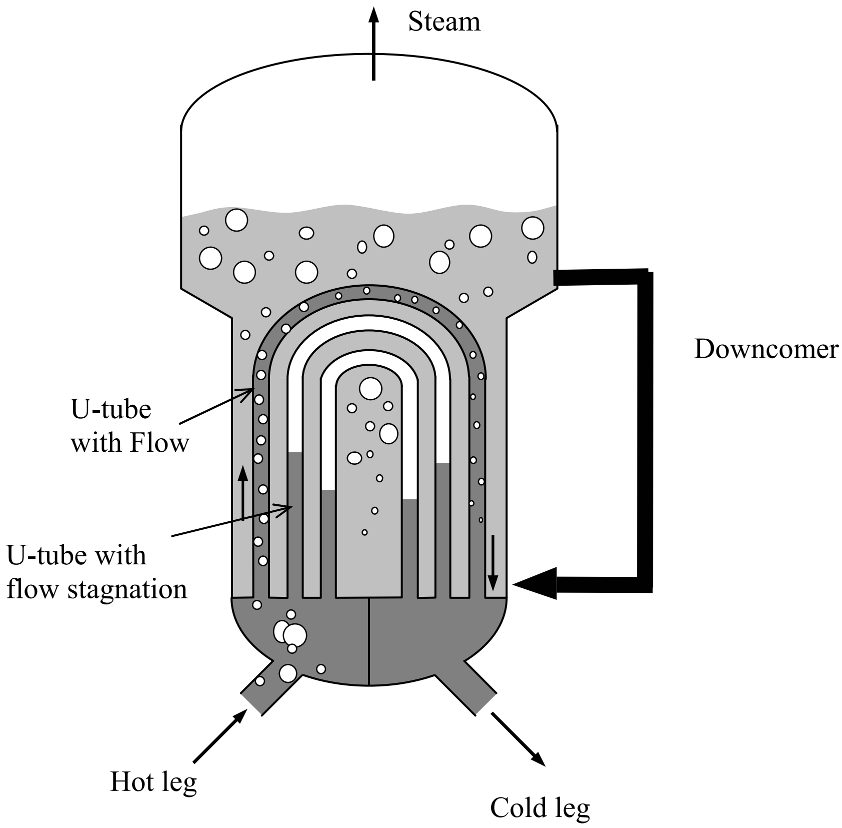

Fig.8 Non-uniform flow behavior at low pressure

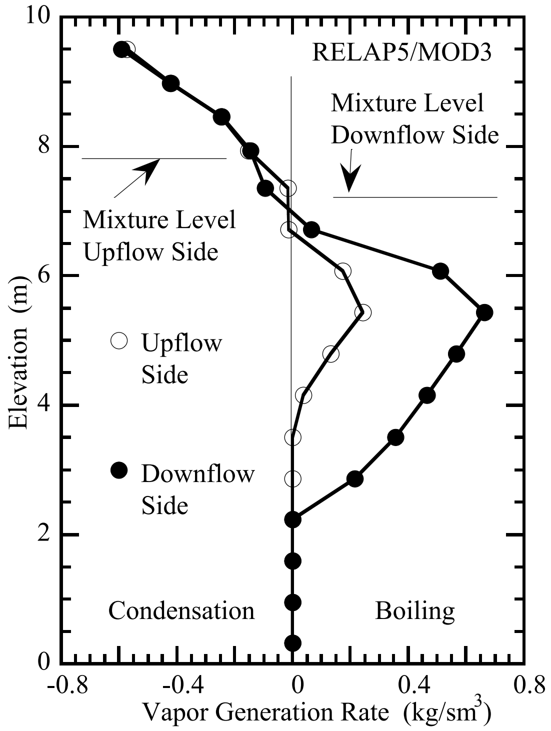

Fig.9 Vapor generation rate distribution in the U-tube with the two-phase stratification, calculated using RELAp5/MOD3

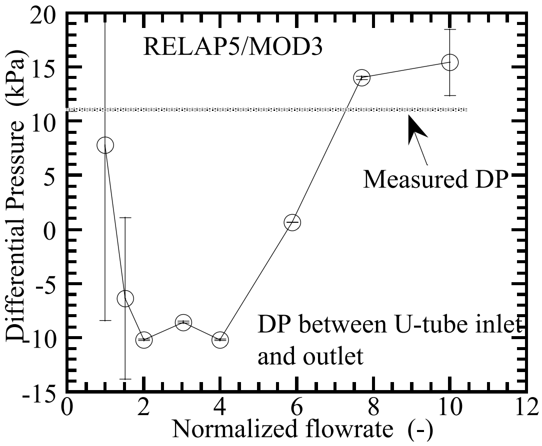

Fig.10 U-tube inlet-outlet differential pressure vs. flow rate calculated using RELAP5/MOD3: Flow rate is normalized by that assuming the uniform distribution among U-tubes.

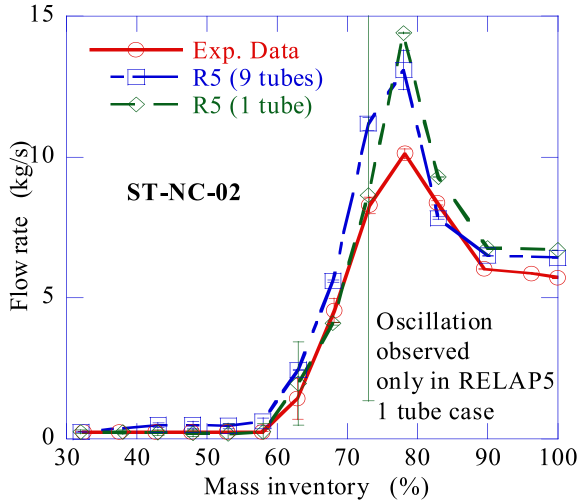

Fig.11 Comparison of loop flow rates vs. mass inventory for high pressure test

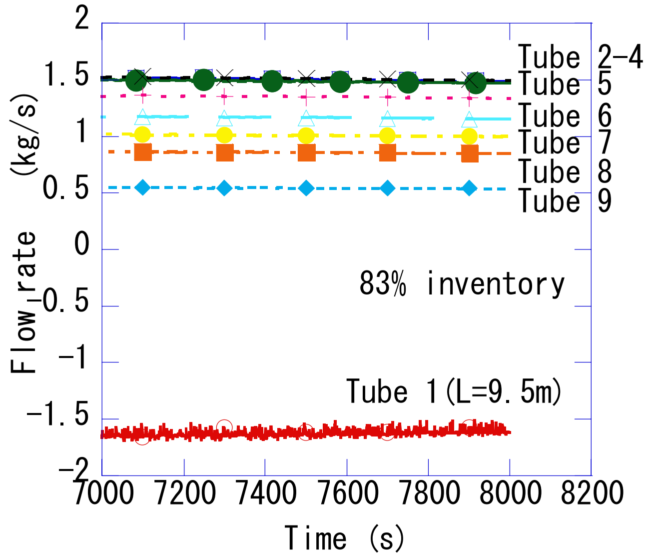

Fig.12 Calculated U-tube flow rate for low pressure test.

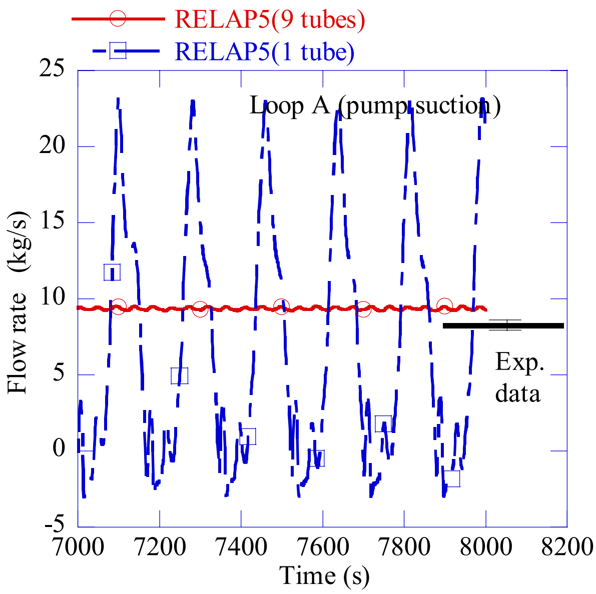

Fig.13 Comparison of loop-A flow rates vs. time for 73% mass inventory for high pressure test

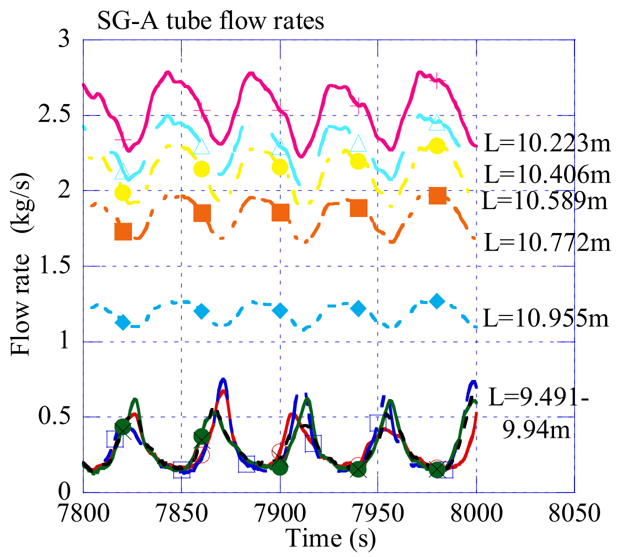

Fig.14 Calculated U-tube flow rates in SG-A for 73% mass inventory for high pressure test

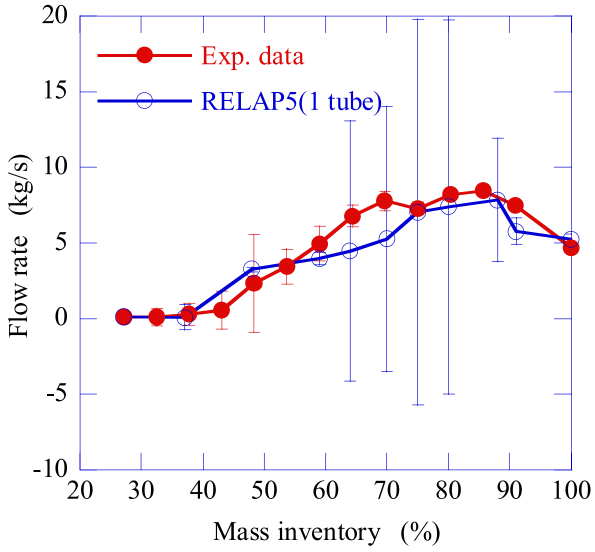

Fig.15 Comparison of loop flow rates vs. mass inventory for low pressure test with one-tube model

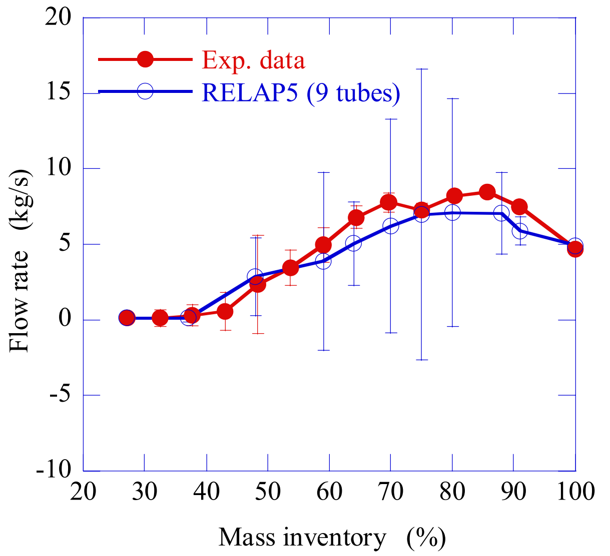

Fig.16 Comparison of loop flow rates vs. mass inventory for low pressure test with nine-tubes model

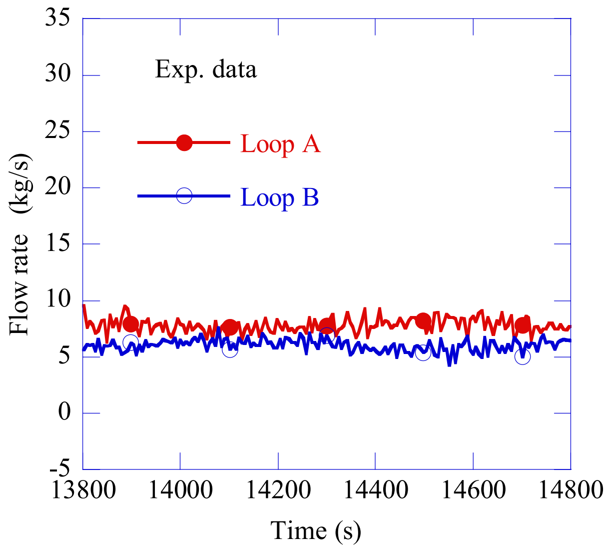

Fig.17 Measured loop flow rates vs. time for 70% mass inventory during low pressure test

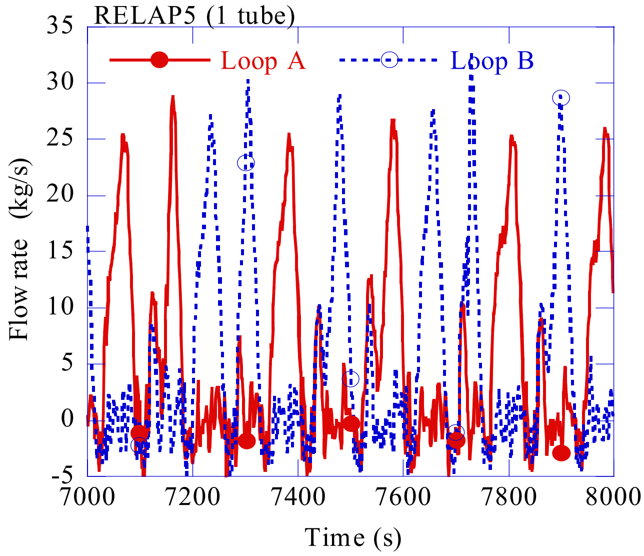

Fig.18 Comparison of calculated loop flow rates vs. time for 70% mass inventory for low pressure test analysis with one-tube model

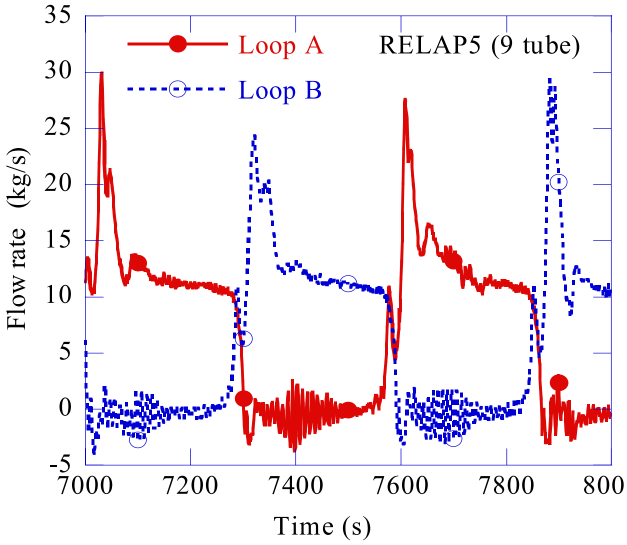

Fig.19 Comparison of calculated loop flow rates vs. time for 70% mass inventory for low pressure test analysis with nine-tubes model

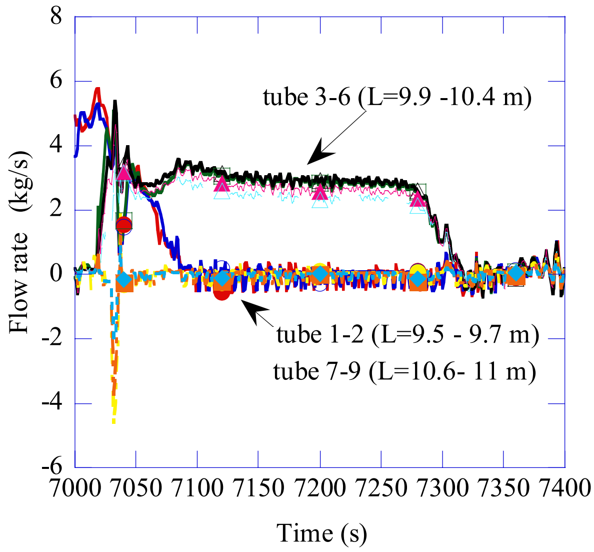

Fig.20 Calculated U-tube flow rates for 70% mass inventory for low pressure test analysis with nine-tubes model

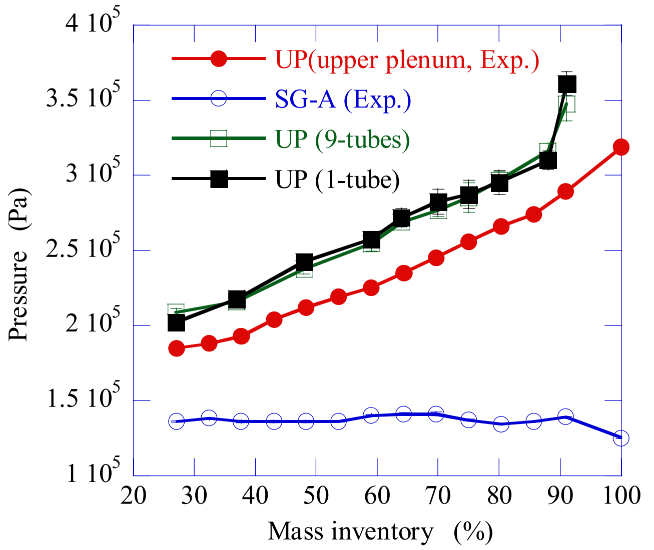

Fig.21 Comparison of pressures between exp. data and RELAP5 analyses for low pressure test